Adsorption of bisphenol A by activated carbon developed from PET waste by KOH activation

Vicente Gómez-Serrano*, Marta Adame-Pereira, María Alexandre-Franco, Carmen Fernández-González

Department of Organic and Inorganic Chemistry, Faculty of Science, University of Extremadura, Badajoz 06006, Spain

Abstract

This study deals with the preparation of activated carbon (AC) from poly(ethylene terephthalate) (PET) waste and with the physicochemical characterization of AC and its use as adsorbent of bisphenol A (BPA) in aqueous solution. AC was prepared by chemical activation with KOH and by physical activation in steam. The activation with KOH was carried out by impregnation first of PET by wet and dry routes at the PET:KOH weight ratios of 1:1, 1:3 and 1:5 and by carbonization then of the resulting products at 850 ºC for 2 h in N_2 atmosphere. The activation in steam was performed by heating at 900 ºC for 1 h. The ACs were characterized by N_2 adsorption at -196 ºC, mercury porosity, mercury density measurements, FT-IR spectroscopy and measurement of pH of the point of zero charge (pH_{pzc}). The activation yield is 58.4-49.4% with KOH in aqueous solution, 75.8-23.9% with solid KOH and 5.9% with steam. Using solid KOH, greater developments of a more heterogeneous porosity with increasing impregnation PET:KOH ratio are achieved. For SK1:5, S_{BET} is 1990 $m^2\ g^{-1}$ and the pore volumes are: 0.71 $cm^3\ g^{-1}$, micropores; 0.81 $cm^3\ g^{-1}$, mesopores; 1.77 $cm^3\ g^{-1}$, macropores. The data of BPA adsorption fit better to the Ho and Mckay second order kinetic model than to the Lagergren first order kinetic model and to the Langmuir equation than to the Freundlich

equation. From the kinetic and thermodynamic standpoints, the adsorption process of BPA is more favourable for SK1:5.

Keywords: PET . KOH activation . Activated carbon . Characterization . Bisphenol A adsorption

---

* Corresponding author: Fax: +34 924 271 149.

E-mail address: vgomez@unex.es (V. Gómez-Serrano).

Introduction

Poly(ethylene terephthalate), commonly abbreviated PET, consists of polymerized units of the ($C_{10}H_8O_4$) monomer ethylene terephthalate (Fig. 1). It is the most common thermoplastic polymer resin of the polyester family. PET is a material that possesses a large number of applications, most of the world´s production being for synthetic fibers (> 60%), plastic bottles (≈ 30%), and industrial uses (≈ 10%) (Ji, 2013). It is most commonly used for packaging of water and carbonated soft drinks. The consumption of PET is steadily increasing in the global plastic market due to the expansion of the PET bottle market. In 2016 it was forecasted that annual PET consumption will be 20 million tonnes by 2021 (Recycling International, 2016). For plastics, in 2017 the production amounted to 348 million tonnes in the world and to 64.4 million tonnes in Europe (PlasticsEurope, 2018). Because PET is one of the most common synthetic polymers used in our daily life, it has become one of the most abundant municipal and industrial wastes. A few decades ago, PET residues on an average were 7.6 wt.% of the different polymer wastes generated in Europe (Brems et al. 2001). The disposal of large quantities of this waste together with its low bio- and photo-degradability represents a serious challenge for industrial countries worldwide. Disposal options include recovery and recycling, landfilling, co-incineration, and thermal processes. Pyrolysis is a thermal process capable of

producing value-added products such liquid and gaseous fuel, monomers, and a carbonaceous residue (char) as a candidate for possible upgrading to activated carbon (AC) or carbon black (Brems et al. 2001).

AC is a porous carbon material used mainly as adsorbent of gases, vapours and water-dissolved chemical substances and also as catalyst and catalyst support. The properties of AC depend on the starting material and the method used in its preparation. Desirable starting materials should contain high carbon content and low inorganic matter content, as gathered in the case of PET. This waste material is further abundantly available in a relatively pure state, which would allow PET-based AC to be produced from a variety of feedstock sources, including engineering and municipal wastes. The use of waste materials such as plastics for AC preparation has been reviewed before (Dias et al. 2007; Bazargan et al. 2013). Using PET as the starting material, AC has been developed by physical activation in various gasification atmospheres (Bóta et al. 1997; László et al. 1999; Kartel et al. 2001; Parra et al. 2002; Nakagawa et al. 2004; Fernández-Morales et al. 2005; Sych et al. 2006; Esfandiari et al. 2012; Bratek et al. 2013) and also by chemical activation (Marzec et al. 1999; Kartel et al. 2001), mainly using KOH as activating agent (Arenillas et al. 2005; Almazán-Almazán et al. 2007; Adibfar et al. 2014; Djahed et al. 2015; Mendoza-Carrasco et al. 2016).

Nowadays, the release of a great variety of organic pollutants of industrial origin to environment is a problem of prime importance because of detrimental and pathological effects. One abundant environmental pollutant is bisphenol A (4,4′-(propane-2,2-diyl)diphenol, BPA), which is an organic compound with two hydroxyphenyl groups and that has the chemical formula $C_{15}H_{16}O_2$ (Fig. 2) BPA is the most typical bisphenol and is one of the most usually produced chemicals worldwide. The annual production of BPA is over three millions tons produced annually (Laing et al. 2016; Hermabessiere et al. 2017). BPA is mainly used as an intermediate in the production of

polycarbonate plastics (65% of volume used) and epoxy resins (30% of volume used), among others, for the lining layer of aluminium cans (Crain et al. 2003). BPA can also be used as other polymers additive (Rani et al. 2015). BPA enters the environment from the discharges of industrial wastewater treatment plants, plastics (i.e., in landfills, industry areas, etc.), processing of BPA in manufacture, and spray paints (Staples et al. 1998; Yamamoto et al. 2001; Cousins et al. 2002; Kamaraj et al. 2012; Lin et al. 2017; Andaluri and Manickavachagam 2018). As a result, it has been detected in all types of environmental water at concentrations ranging from 17.2 mg L^{-1} in hazardous waste landfill leachate (Yamamoto et al. 2001) to 12 µg L^{-1} in stream water (Liu et al. 2009) and 3.5–59.8 ng L^{-1} in drinking water (Santhi et al. 2012).

Presently, it is well established that there is ubiquitous human exposure to BPA (Le et al. 2009). Food and beverage have been identified as the major sources of human exposure to BPA. Thus, as previously reported (Wagner and Oehlmann 2009; Colin et al. 2014), BPA leaches out into bottled mineral water. For polycarbonate bottles, the migration of BPA occurs at rates ranging from 0.20 to 0.79 ng per hour (Le et al. 2007). Also, it may migrate from interior can coating and polycarbonate containers under acidic conditions or thermal heat treatment in processing. Due to its potential health risk, in 1986 the European Union through the Scientific Committee on Food (SCF) allocated a Tolerable Daily Intake (TDI) for BPA at the level 50 µg/kg bw/day. In 2011, the Commission Directive 2011/8/EU prohibited the manufacture of polycarbonated infant feeding bottles with BPA and the import into the EU of such feeding bottles. In 2015, the TDI was lowered down to 4 µg/kg bw/day (Cwiek-Ludwicka 2015). In the United State, the Food and Drug Administration (FDA) banned the use of BPA in baby bottles and cups in 2012.

As is well known, most environmental organic pollutants are Endocrine Disruptors Chemicals (EDCs) as they interfere with the endocrine system. BPA is an endocrine disruptor for humans and animals, showing estrogenic activity even at concentrations below 1 ng L^{-1} (Rykowska and Wasiak 2006; and refers therein). Because of its widespread use and growing evidence that may adversely affect human health (Rochester 2013), the fate of the environmental BPA is an issue of increasing social concern. Accordingly, there is current interest in setting up methods to achieve a fast and effective removal of BPA from various exposure sources. In heavily populated areas or industrial sites the contamination by EDCs affects the surface and profound water systems, the surrounding land and drinking waters. To clean chemically polluted water, conventional methods include reverse osmosis, chemical precipitation, electrochemical treatment, evaporative recovery, ion exchange and adsorption (Pellera et al. 2012). BPA degradation by advanced oxidation processes (i.e., ozonation, dark- and photo-Fenton oxidation, ultrasound irradiation, and so on) were reported to be effective methods in the removal of EDCs, their low-cost effectiveness in dealing with large volume of low-level pollutants and risk of generation of toxic by-products constituting major barriers in the field of applications (Zielinska et al. 2018). Adsorption was recognized by the Environmental Protection Agency (EPA) as one of the best methods available to remove organic and inorganic compounds from water intended for human consumption. As the adsorbent, among the various available materials used more frequently with time, activated carbon (AC) has been one of the most important materials from an industrial point of view. In fact, AC is a unique and nearly universal adsorbent for such a purpose due to its textural properties and surface chemistry, as it possesses a large surface area and well-developed internal micropore structure as well as a wide spectrum of surface functional groups (Radovic et al. 2001; Bautista-Toledo et al. 2014).

In the light of the foregoing, the main objectives of this study were: (1) from a highly deleterious environmental pollutant as PET plastic bottles to prepare AC beneficially intended for use as adsorbent of a water ubiquitous noxious pollutant as BPA, which may be further generated from plastic bottles, (2) to optimize the preparation process of AC by activating with KOH as compared to steam, and (3) to test selected AC samples in the adsorption of BPA in aqueous solution. The adsorption process of BPA was studied from the kinetic and equilibrium standpoints.

Materials and methods

Raw material

Postconsumer 5 L mineral water bottles were used as the PET source. The plastic bottles were first greatly size-reduced by cutting them with laboratory scissors to ≈ 0.5 cm side squared pieces, which were chosen for subsequent studies. After that, the plastic material was analysed in a LECO CHNS-932 equipment and incinerated at 650 ºC for 12 h in a muffle furnace. The resulting compositional data are: C, 62.9%; H, 4.3%; N, 0.0%; S, 0.0%, and ash content, 0.0%. As obtained by difference, the oxygen content is equal to 32.9%. The calculated contents of C, H and O from the chemical formula of PET are in turn 62.5%, 4.2% and 33.3%. All reagents were analytical grade, being used without further purification. Potassium hydroxide (85%, Panreac, Barcelona, Spain) and BPA (Merck) were used.

Preparation of AC

The preparation of AC from PET was undertaken by activation mainly with KOH and marginally in steam, for comparison purposes. In previous studies, the impregnation of PET with KOH was carried out using given amounts of PET and KOH in aqueous solution at the PET:KOH weight

145 ratios 1:1 (Adibfar et al. 2014), 1:4 (Arenillas et al. 2005) and 1:6 (Almazán-Almazán et al.
146 2007) or solid KOH at the PET:KOH weight ratios 4:1 (Djahed et al. 2015) and 1:2 (Mendoza-
147 Carrasco et al. 2016). Here, specifically, KOH was used both in aqueous solution, by allowing
148 for that PET suffers alkaline hydrolysis (Paszun and Spychaj 1997; Kaufman et al. 1999; Wan
149 et al. 2001; Karayannidis et al. 2002; Kumar and Guria 2005; Spaseska and Civkaroska 2010;
150 Yamashita and Mukai 2011), and as the commercially furnished solid product at three
151 impregnation PET:KOH weight ratios. In the wet impregnation of PET, 20 g of PET and 250
152 mL of KOH solution under steady mechanical agitation were maintained in contact at 85 °C for
153 2 h. Next, the supernatant liquid was separated by vacuum filtration and the remaining solid
154 was oven-dried at 120 °C for 24 h. In the dry impregnation, 2 g of PET and the corresponding
155 amounts of KOH were physically mixed for homogenization, as far as possible. The resulting
156 two series of KOH-impregnated products are noted as LK and SK. For the activation treatments,
157 about 5 g of KOH-impregnated product or PET depending on the activation method were used.
158 Further details of the methods used in the preparation of AC were given in a previous report
159 (Mendoza-Carrasco et al. 2016). Operational conditions are summarized in Table 1 together
160 with sample notations. The yield values for the impregnation and activation processes were
161 calculated by the expression (1),

162 $$\text{Yield } (I_Y, A_Y) = \frac{M_{FM}}{M_{SM}} \text{ x } 100 \qquad (1)$$

163 where M_{SM} is the starting mass of PET or PET-impregnated product and M_{FM} is the final mass
164 of impregnated product or AC and listed in Table 1.

165 **Textural characterization and surface chemistry of AC**

166 The characterization of the samples was accomplished by N_2 adsorption at -196 °C, mercury
167 porosimetry, mercury density measurement, FT-IR spectroscopy, and measurement of pH of

the point of zero charge (pH_{pzc}), as described in full detail in a previous study (Mendoza-Carrasco et al. 2016).

Adsorption of BPA

In the study of the adsorption process of BPA in aqueous solution only WV and the SK samples were used as adsorbents since, as shown by preliminary results, adsorption was practically negligible with the LK samples. BPA adsorption tests were carried out by the batch procedure by using a Selecta thermostatic shaker bath (Unitronic-ORC) with water at 25 °C and shaken at 50 oscillations per minute. The concentration of the BPA solution and the amount of adsorbent used in the adsorption tests were chosen by taken into account that BPA is moderately soluble in water, i.e., 300 mg L^{-1}/1.31 x 10^{-3} mol L^{-1} at room temperature (Rykowska and Wasiak 2006). Accordingly, a 10^{-3} mol L^{-1} BPA stock solution was prepared for such a purpose. pH of such a solution was 6.22, as measured in a Crison pH-Meter 21. The reported pK_a1 and pK_a2 for the BPA dissociation to an anionic or di-anionic species are 9.6 and 10.2 (Staples et al. 1998; Tay et al. 2012). In a typical kinetic experiment, ≈ 0.01 g of adsorbent and 25 mL of the BPA stock solution were added to a set of 25 mL glass test tubes, provided with Bakelite screw-up caps, and kept in contact for a time between 1 min and several days. In the equilibrium experiments, however, the amount of adsorbent placed in each test tube ranged between 0.008 g and 0.02 g and the adsorption time was long enough to reach equilibration in the system.

The BPA solutions were analysed by UV-Vis spectrophotometry in an UV-1800 Shimadzu equipment. After recording the absorption spectrum of BPA in such spectral regions to know the maximum absorbance wavelength for BPA, it was checked first that BPA is stable in aqueous solution for longer than necessary for a typical adsorption kinetic or equilibrium experiment. Then it was also verified that the absorbance against concentration data obey well

the Beer´s law, absorbance measurements being effected thereafter at 276 nm. The adsorption of BPA was quantified using the following mass balance equation:

$$q_e = (C_i - C_f)V/W \quad (2)$$

where q_e stands for the amount of BPA adsorbed per unit weight of adsorbent, C_i and C_f are the initial and final concentrations of BPA, V is the solution volume (L) and W is the adsorbent weight.

Study of BPA in the adsorbed state

To get some insight into the interaction of CA and BPA and into the adsorption mechanisms, an aliquot of the stock solution of BPA was maintained in contact with SK1:5 for 5 days and once this time had elapsed the residual liquid was filtrated and the remaining solid was oven-drying at 110 ºC overnight. The resulting product (SK1:5-BPA, hereafter) was analysed by FT-IR spectroscopy as for the AC samples. This also applies to solid bisphenol A, the spectrum of which was registered for comparison purposes.

Results and discussion

Preparation of AC. Process yield

Wet impregnation stage

The yield values for the impregnation process of PET (Table 1) show that the PET mass noticeably decreased after the contact with the KOH aqueous solutions. Also, notice that the mass decrease was significantly higher with increasing impregnation ratio. Probably, the main factor influencing the mass of sample was the alkaline hydrolysis of PET, i.e., ester bonds of PET are cleaved by the nucleophilic attack of hydroxide ions under the formation of the di-potassium terephthalate salt and ethylene glycol, which are both soluble in the aqueous phase

(Palme et al. 2017). In fact, ethylene glycol is miscible with water. In connection with the alkaline hydrolysis of PET it has been stated previously that almost complete conversion of PET occurs in relatively mild process conditions. Thus, it leads to the total depolymerisation of PET to its monomers in reaction times ranging from a few to 30 min at high temperature and under high pressures, and requires no additives, such as catalysts or neutralizers (Spaseska and Civkaroska 2010; and refers therein). Nevertheless, heat treatment temperatures between 120 and 200 ºC and reaction times of 1-7 h have been reported before (Karayannidis and Chatziavgoustis 2002). The less severe heating conditions of 85 ºC for 2 h at atmospheric pressure used when PET was chemically treated with the KOH aqueous solutions can account for the high yields in the range ≈ 96-76% obtained in this study. The increase produced in the mass loss of PET with increasing PET:KOH ratio is consistent with the stoichiometry of the hydrolysis reaction, which takes place between two moles of KOH and one mole of BPA and that therefore was more favourable with a greater presence of KOH in the reaction medium. Therefore, only when the PET:KOH ratios of 1:3 and 1:5 were used, KOH was really in excess with respect to PET. Since after soaking at 85 ºC for 2 h the residual aqueous liquid was separated from the remaining solid by filtration, it becomes apparent that the unreacted KOH to a large extent was removed as contained in the filtrate. Finally it should be mentioned that, based on alkaline hydrolysis of PET, a method of preparation of AC has been developed before consisting of the stages of PET complete de-polymerization, filtration, water evaporation, and solid carbonization (Almazán-Almazán et al. 2007).

Activation stage

In the case of the activation stage, mass balance data (Table 1) show that yield is strongly dependent on the method used in the overall process of preparation of AC from PET. First, yield is much higher when it was carried by chemical activation with KOH than by physical activation in steam. Second, it is noticeably dependent on whether the impregnation was

effected by the wet or dry route according to the PET:KOH ratio; being higher and lower at a low and at higher impregnation ratios, respectively. Third, yield greatly decreases with increasing impregnation ratio, being as low as 23.9% at most for SK1:5. Nevertheless, this yield is however significantly higher than 17.1% obtained for the pyrolysis of PET at 900 ºC for 2 h in N_2, which was performed in an aside experiment. Furthermore, it is worth noting that the yield of 38.1% for SK1:3 compares with yields obtained for the preparation of AC from a lignocellulosic material as cherry stone by chemical activation with H_3PO_4 (Olivares-Marín et al. 2007). Since AC is frequently prepared from woody materials it is also relevant to point out here that the yield of the carbonization of cherry stones, which followed by the activation of resulting product, was 26.3 and 25.4 % when heating from ambient temperature to 600 ºC in the atmosphere of the pyrolysis products and in N_2, respectively (Durán-Valle et al. 2005). Therefore, the relatively high yield obtained for the preparation of AC from PET is an interesting finding as the economic analyses of AC plants are very sensitive to activation route and production yield (Bazargan et al. 2013).

Textural characterization

Surface area, micro- and mesoporosity

The adsorption isotherms of N_2 at -196 ºC measured for the various AC samples, which were prepared as described above, are shown in Fig. 3. In accordance with the BDDT classification system based on the shape of the N_2 isotherm, the aforesaid isotherms resemble composite Type I and IV isotherms for WV and the SK samples and Type II and IV isotherms for the LK samples, and therefore adsorption must occur in micro- and mesopores and on external surface and in large size pores, respectively. From the variation of the volume of N_2 adsorbed at low p/p^0 values (i.e., up to 0.2-0.3), or in other words from the isotherm knees, it follows that the micropore size distribution is wider by SK1:5 > SK1:3 > WV > SK1:1. In the mesopore range,

however, porosity is more heterogeneous by SK1:5 > WV > SK1:3 ≈ SK1:1. Therefore, it may be stated that the increase in the PET:KOH ratio used in the impregnation of PET originated porosity widening. As shown by the values of S_{BET} and pore volumes obtained from the N_2 isotherms (Table 2), S_{BET} and W_0 are much higher for SK1:5 than for WV but similar for SK1:1 and WV. Furthermore, S_{BET} and W_0 are as high as 1990 m^2 g^{-1} and 0.71 cm^3 g^{-1} for SK1:5 and by contrast as low as 12 m^2 g^{-1} and 0.0 cm^3 g^{-1} for LK1:5. For ACs prepared by wet impregnation of PET with KOH, S_{BET} was between 472 and 1391 m^2 g^{-1} (Arenillas et al. 2005; Almazán-Almazán et al. 2007; Adibfar et al. 2014), which are by far lower than 1990 m^2 g^{-1} for SK1:5 and that prove the use of solid KOH in the preparation of AC had a marked beneficial effect on the creation of microporosity. Moreover, S_{BET} and W_0 greatly increase with increasing KOH content in the impregnation mixture, which is also worthy to be highlighted. In summary, from the results obtained in the textural characterization of AC by N_2 adsorption at -196 ºC it follows therefore that the degree of development of the surface area and microporosity is larger by activating with solid KOH than in steam and by using solid KOH instead of KOH in aqueous solution in the impregnation of PET and also by increasing the content of solid KOH in the impregnation mixture. In brief, the textural effects associated with the activation process of PET or KOH-impregnated PET are more favourable by the order SK > WV >> LK and SK1:5 > SK1:3 > SK1:1.

Meso- and macroporosity

The curves of mercury intrusion obtained for the samples are plotted in Fig. 4. It is shown that the pore size distribution in the region of macro- or mesopores is wider for the SK samples and for SK1:5 and WV, respectively. Also, it is worthwhile noting the presence of varying size macropores in the LK samples. Likewise, regarding mesoporosity, the results of mercury porosimery are well in agreement with those of N_2 adsorption at -196 ºC, as far as the pore size distribution of SK1:5 and WV is concerned. As can be seen in Table 3, $V_{me\text{-}p}$ is 0.81 cm^3 g^{-1} for

290 SK1:5 and V_{ma-p} is 2.11 cm^3 g^{-1} for SK1:3. For the LK samples, however, V_{me-p} and V_{ma-p} are
291 at most 0.13 and 0.38 cm^3 g^{-1} in the case of LK1:1. Such samples, in general, are by far more
292 macroporous than mesoporous ACs. The opposite applies to WV as V_{me-p} is 0.36 cm^3 g^{-1} and
293 V_{ma-p} is 0.08 cm^3 g^{-1} for this sample. In short, from the above results of N_2 adsorption and
294 mercury porosimetry it becomes apparent that by using PET as feedstock the preparation of AC
295 with a more or less heterogeneous porosity by SK samples > WV > KL samples is feasible,
296 which is an interesting finding with a view to preparing AC with a tailored porous structure.

297 **Total porosity**

298 The mercury density (ρ_{Hg}), or apparent density, of a solid is the weight of one millilitre of solid
299 granules, excluding the volume of the interstitial space between them (Smisek and Cerny 1970).
300 Therefore, the value of ρ_{Hg} (g cm^{-3}), or better of ρ_{Hg}^{-1} (cm^3 g^{-1}), may be regarded as a rough
301 estimate of the total porosity present in a porous solid, embracing even narrower pores that are
302 not accessible to small gas molecules, such a He and N_2. Although mercury does not wet porous
303 solids such as AC, the use of ρ_{Hg} for such as purpose is somehow handicapped by the presence
304 of large size pores which are filled with mercury prior applying pressure in the porosimeter.
305 The reported ρ_{Hg} densities are usually from 0.6 to 0.8 g cm^{-3} (Smisek and Cerny 1970). Data in
306 Table 3 show in fact that ρ_{Hg} is notably higher for the LK samples than for the SK samples,
307 which is in line with the highly uneven porosity development in both series of samples. This is
308 also evident from the V'_T values (Table 3), which range between 0.43 and 0.57 cm^3 g^{-1} for the
309 former samples and between 2.21 and 3.29 cm^3 g^{-1} for the latter samples. The so high ρ_{Hg}
310 measured for WV appears to be striking as V'_T is 0.91 cm^3 g^{-1} for this sample, which is markedly
311 higher than for the LK samples and lower than for the SK samples. However, it is worth noting
312 that the values of ρ_{Hg}^{-1} and V'_T are fairly close for WV and the SK samples, in particular for
313 SK1:3 with ρ_{Hg}^{-1} and V'_T equal to 3.23 cm^3 g^{-1} and 3.25 cm^3 g^{-1}, respectively. The much higher

314 ρ_{Hg}^{-1} than V'_T for the LK samples argues for an important presence of small pores in the LK
315 samples, which are not accessible to N_2(g) at -196 ºC.

316 **Surface chemistry study**

317 **By FT-IR spectroscopy**

318 The FT-IR spectra registered between 4000 and 400 cm^{-1} for WV, SK1:3 and SK1:5 (Fig. 5)
319 show a series of stronger absorption bands of varying intensity with their absorption maximum
320 located in the neighbourhood of 3700, 1675, 1460 (i.e., this band is broad and has a shoulder at
321 higher frequencies) or 1014 cm^{-1}, which are ascribable in turn to the ν(O-H) vibration of
322 hydroxyl groups, ν(C=O) vibration of quinone type structures rather than to the same bond
323 vibration mode in carboxylic acid groups, ν(C=C) skeletal of aromatic rings and $\delta_a(CH_2)$ of –
324 CH_2- groups, ν(C-O) vibration of hydroxyl groups/ether type structures. Notice that only the
325 spectrum of WV displays the broad band around 3431 cm^{-1}. This band can also be assigned to
326 the ν(O-H) vibration of hydroxyl groups which are probably involved in hydrogen bonding. On
327 the other hand, the weak bands at 2932 and 2860 cm^{-1} are readily visible only in the spectra of
328 WV and SK1:3, being attributable to the ν_a(C-H) vibration and ν_s(C-H) vibration of -CH_2-
329 groups. Band intensities indicate a greater presence of H-bonded –OH groups and –CH_2–
330 groups in WV and of C=O groups and C=C bonds containing rings in SK1:3 and especially in
331 SK1:5. Symbols mean: ν, stretching, δ, bending; a, asymmetrical; s, symmetrical.

332 **By pH_{pzc} measurement**

333 From the plot of pH of the initial solution of BPA (pH_i) against pH of the supernatant (pH_f)
334 (Fig. 6), the pH_{pzc} values given in Table 4 were obtained for the samples. As can be seen, pH_{pzc}
335 is slightly higher or lower than 7.0, which is consistent with the presence of weak acidic –OH
336 surface groups in the samples analysed by FT-IR. Furthermore, pH_{pzc} varies by WV (7.20) >

LK samples (≈ 6.35-6.25) > SK samples (≈ 5.70-5.35). The sequence of pH_{pzc} variation must be kept in mind in connection with the results of BPA adsorption since the pH_{pzc} value indicates the pH at which the surface of an AC changes its charge from positive to negative, which must influence the adsorption of charged adsorptives from aqueous solution.

FT-IR spectrum of SK1:5-BPA

The FT-IR spectrum registered for SK1:5-BPA is plotted in Fig. 7, together with those for BPA and SK1:5 which have been also included for comparison purposes. As can be seen, the spectrum of BPA in the range of wavenumbers between 400 and 4000 cm^{-1} displays a number of spectral features which are assigned as shown in Table 5. In connection with the spectrum of SK1:5-BPA, it is worth noting that all absorption bands appearing in the spectra of BPA and SK1:5 are readily visible in the spectrum of SK1:5-BPA. In this spectrum, as the most noticeable change, it is noted that the bands around 1605 and 1500 cm^{-1} in relative terms undergo a significantly decrease in intensity with regard to the band at 1377 cm^{-1}.

Adsorption of BPA

Kinetics

The plots of concentration (C, mol L^{-1}) vs. time (t, h) obtained for the adsorption of BPA by the selected AC samples are depicted in Fig. 8. They show first that most BPA adsorbed at short adsorbent-adsorptive contact times, especially in the case of SK1:5 and SK1:3. For WV, however, the variation of C is clearly more significant until somewhat longer times. In any event, at times greater than 50 h adsorption was practically negligible for all adsorbents. Secondly, it should be noted that after a few hours of BPA adsorption the extent to which it occurred was markedly larger for SK1:5 and SK1:3 than SK1:1 and WV, i.e., the concentration decrease produced in the BPA solution was as high as ≈ 70% for SK1:5 and SK1:3, whereas

for SK1:1 and WV it was ≈ 30%. Accordingly, the adsorption process of BPA was faster for SK1:5 and SK1:3 than for SK1:1 and in particular for WV. Regarding kinetics, the behaviour of the AC samples in the adsorption of BPA is consistent with the degree of mesoporosity development. Thus, $V_{me\text{-}p}$ is noticeably higher for SK1:5 and SK1:3 than for SK1:1 and WV (Table 3), while V_{me} is higher for WV as compared to SK1:1 and SK1:3 (Table 2). In fact, as is well known, mesopores control the internal diffusion of the adsorptive towards the micropores, which is where most adsorption active sites concentrate in adsorbents with a high surface area as AC. However, the pore size distribution of the adsorbents in the region of mesopores does not seem to play a prominent role in the kinetics of the adsorption process of BPA as mesoporosity is more heterogeneous not only in SK1:5 but also in WV than in SK1:3 and SK1:1 (Fig. 4). Nevertheless, the presence of larger micropores in the adsorbents as SK1:5 may render narrower pores more easily accessible to BPA. Also, macroporosity is much better developed in the products of PET activation with solid KOH than in steam atmosphere.

The kinetic data was fitted to the Lagergren equation (pseudo-first order kinetic model) and to the Ho and Mckay equation (1999) (pseudo-second order kinetic model). The integrated Lagergren equation in linear form is:

$$\log(q_e - q_t) = \log q_e - \frac{k_1}{2.303} t \qquad (3)$$

where q_t and q_e are the amounts adsorbed at time t and at equilibrium (mole g^{-1}), respectively, and k_1 is the pseudo-first order rate constant (h^{-1}). The plot of log (q_e–q_t) versus t should therefore be a straight line with slope log q_e and intercept $–k_1/2.303$.

The pseudo-second order equation is:

$$\frac{t}{q_t} = \frac{1}{k_2 q_e^2} + \frac{1}{q_e} t \qquad (4)$$

where q_e and q_t are the adsorption capacities at equilibrium and time t, respectively (mol g^{-1}) and k_2 is the rate constant of pseudo-second order adsorption (g mol^{-1} h^{-1}). Here, the plot of t/q_t against t should give a linear relationship, which enables to obtain q_e and k_2 from the slope and intercept of the plot.

The calculated values of q_e, k_1, k_2 and R^2 are listed in Table 6. From the values of R^2 it follows that the kinetic data fitted better to the pseudo-second order kinetic model than to the pseudo-first order kinetic model. Furthermore it is seen that k_2 varies by SK1:5 > SK1:1 > SK1:3 > WV. As expected, k_2 is markedly lower for WV than for the rest of samples. However, the smaller value of k_2 for SK1:3 than for SK1:1 seems to be striking if one allows for the textural properties of both samples, as described above.

Adsorption isotherms

The adsorption isotherms measured for the AC samples and BPA in dilute aqueous solution are plotted in Fig. 9. At a glance they show that, practically in the entire range of C_e/C_0 (i.e., C_e and C_0 are the equilibrium and initial concentrations of BPA), adsorption was higher by SK1:5 > SK1:3 > WV > SK1:1. Furthermore, it is substantial at C_e/C_0 = 0.0 and increases at higher C_e/C_0, but especially above C_e/C_0 > 0.8 for a larger number of samples. A well-defined long isotherm plateau is not observed for most samples, except for SK1:1. Regarding the isotherm shapes, they resemble the H curve of the Giles´s classification system of solution adsorption systems (Giles et al. 1960). Therefore, it is indicative of a high affinity of the solute in a dilute solution for the adsorbent in such a way that it is completely adsorbed at low C_e/C_0 and also that adsorption is flat. This adsorption instead of end-on on the surface of narrow pores as the micropores, which are less than ≈ 20 Å in width (Gregg and Sing 1982), is consistent with the geometry of the BPA molecule, i.e., 3.83, 5.87 and 10.68 Å (Schäfer et al. 2006). It is further supported by the measured pH_{pzc} for the adsorbent samples (Table 4) and by pH of the BPA

406 solution and pK_a of BPA dissolved in water, as mentioned above. Furthermore, pH only
407 increased slightly after the adsorption process of BPA. Correspondingly, both the surface
408 groups and structures of the adsorbent and BPA are both slightly acidic in character and
409 therefore they would remain practically undissociated after the contact of the BPA solution with
410 the adsorbent was established. Consequently, the hydrophobic and π-π molecular interactions
411 should prevail over the ion-ion electrostatic interactions, BPA becoming adsorbed then flat.
412 Adsorption may occur because of the interactions between hydrophobic groups/hydrophilic
413 groups (i.e., see schematically for ibuprofen, Dwivedi et al. 2011) and electron-donating-
414 nucleophilic groups/electron-withdrawing-electrophilic groups of AC and BPA. When
415 studying the adsorption of bisphenol A on lignin, it was stated by Han et al (2012) that the π-π
416 interaction between lignin and BPA contribute importantly to adsorption due to the aromatic
417 ring with hydroxyl group of BPA is a π donor and the lignin acts as an π acceptor. For SK1:5
418 and BPA, it is probable that non-covalent π-π interactions were also involved in the adsorption
419 process, as proved by the results of FT-IR spectroscopy obtained in the present study. Such
420 interactions should influence first the orientation of BPA on the surface of the adsorbent and
421 then, under infrared radiation, bond vibration modes of BPA in the adsorbed state. The latter is
422 shown by decrease produced in ν(C=C) skeletal vibrations of BPA after its adsorption by SK1:5
423 (sample SK1:5-BPA), as inferred from the infrared spectra obtained for BPA, SK1:5 and
424 SK1:5-BPA (Fig. 7). Of course, the mitigation of vibration modes would be only possible
425 provided that the surface orientation of BPA was flat.

426 A short isotherm plateau must mean that the adsorbed solute molecules expose a surface
427 which has nearly the same affinity as the original surface had. Moreover, the second adsorption
428 rise, which starts at a very different C_e/C_0 depending on the sample, argues for multilayer
429 adsorption or on fresh surface (Giles et al. 1960). Multilayer adsorption would be a more

favourable process by SK1:5 > SK1:3 > SK1:1 ≈ WV due to the progressive increase produced in the size of micropores from SK1:1 and WV to SK1:5 in the series of samples (see Fig. 3).

From the data of adsorption equilibrium for BPA, i.e., $q_e=f(C_e/C_0)$, it is possible to obtain valuable information about the adsorption process. For this purpose, the adsorption isotherm is adjusted to different theoretical models in order to offer the parameters of the process which allow characterization and to establish comparisons deemed appropriate. In the present study, the aforesaid data were fitted according to the Langmuir and Freundlich equations. The Langmuir model has been widely used to describe the monolayer adsorption occurring on homogenous surface with a finite number of identical adsorption sites, which can be represented by the following equation:

$$q_e = \frac{Q_0 b C_e}{1+bC_e} \quad (5)$$

where q_e is the amount of BPA adsorbed per unit mass of adsorbent (mol g^{-1}), C_e is the equilibrium concentration of the adsorptive solution in contact with adsorbent (mol L^{-1}), Q_0 the monolayer adsorption capacity (mol g^{-1}) and b a constant related to the free adsorption energy ($b \propto e^{-\Delta H/RT}$). Frequently, equation (5) is rearranged in the form:

$$\frac{C_e}{q_e} = \frac{1}{Q_0 b} + \frac{C_e}{Q_0} \quad (6)$$

the plot of C_e/q_e (g L^{-1}) versus C_e (mol L^{-1}) should give a linear relationship, from which $1/Q_0$ and $1/Q_0b$ can be obtained from the slope and intercept of the plot.

One of the major characteristics of the Langmuir isotherm is that may be expressed in terms of equilibrium parameter (R_L), which is a dimensionless constant referred to as separation factor or equilibrium parameter, defined by Weber and Chakravorti (Weber 1974) as:

$$R_L = \frac{1}{1+bC_0} \quad (7)$$

where b is the Langmuir constant and C_0 is the initial concentration of the adsorbate solution. R_L value indicates the adsorption nature: unfavourable if $R_L>1$, linear if R=1, favourable if $0 < R_L < 1$ and irreversible if $R_L=0$.

The Freundlich isotherm was one of the first equations proposed to associate the adsorbed amount of a chemical species by a given amount of adsorbent with the concentration of that species in the solution. These data often fit the next equation put forward by Freundlich at the beginning of the last century:

$$q_e = K_F C_e^{\frac{1}{n}} \quad (8)$$

where q_e is the amount retained of solute per gram of the adsorbent (mol g^{-1}) at equilibrium, C_e is the equilibrium concentration (mol L^{-1}), K_F and 1/n ($0 < 1/n < 1$) are constants related to the adsorption capacity of the adsorbent and the adsorption intensity. The values of these constants can be obtained from the following expression:

$$\log q_e = \log K_F + \frac{1}{n}\log C_e \quad (9)$$

with 1/n and K_F being computed from the slope and intercept of the Freundlich plot of log q_e against log C_e.

The resulting values of the isotherm parameters of Langmuir and Freundlich (n, K_F, Q_0, b) and fitting coefficient (R^2) are listed in Table 7. From the values of R^2 it follows that the adsorption isotherms of BPA as a rule fits more satisfactorily to the Langmuir isotherm model than to the Freundlich isotherm model, except for SK1:1. It was expected in view of the PET chemical composition since it is constituted of carbon, hydrogen and oxygen and by thermal decomposition should become transformed into a product with a very homogeneous surface.

Furthermore, R_L is > 0 and < 1 and further low and therefore the adsorption process appears to be favourable and rather irreversible. Moreover, Q_0 varies by SK1:5 > WV > SK1:3 > SK1:1, as inferred also from the adsorption isotherms determined for BPA (Fig. 9).

The adsorption capacity of BPA by mineral and carbonaceous adsorbents of various origins has been reviewed before by Dong et al. (2010) and by Han et al. (2012). For comparison purposes, the values of S_{BET}, micropore volume (V_{mi}) and total pore volume (V_t) together with those of the Langmuir adsorption capacity of BPA obtained using AC adsorbents for BPA are collected in Table 8. From this table it is follows that SK1:5 is the AC with a better development of surface area and microporosity and more effective as adsorbent of BPA. By taking also into account the absence of inorganic matter from PET, it may be stated that PET is a good raw material to prepare AC adsorbents for the adsorption of BPA in aqueous solution.

Conclusions

From the results obtained in the present study, focused on the preparation of AC from PET waste by activation with KOH and in steam and on the physiochemical characterization of the resulting AC and its use as adsorbent of BPA in aqueous solution, the following conclusions may be drawn. The yield of the process of preparation of AC from PET by KOH activation is high, regardless of whether impregnation is effected by the wet or dry route. Activation yield ranges between 23.9% and 75.8% with KOH, whereas in steam it is ≈ 6.0%. The beneficial textural effects associated with the process of preparation of AC are by far stronger when solid KOH is used as activating agent, as compared to KOH in aqueous solution or steam, and depend on the impregnation PET:KOH ratio. By activating with solid KOH, AC with a heterogeneous porosity in the regions of macro-, meso- and micropores is prepared. In the micropore range,

the pore size distribution is wider with increasing impregnation ratio. For SK1:5, S_{BET} is 1990 $m^2\ g^{-1}$ and the pore volumes are equal to 0.71 $cm^3\ g^{-1}$(W_0), 0.81 $cm^3\ g^{-1}$ (V_{me-p}), 1.77 $cm^3\ g^{-1}$ (V_{ma-p}) and and 3.29 $cm^3\ g^{-1}$ (V'_T). In the case of WV, as a guide, S_{BET} is 1061 $m^2\ g^{-1}$ and W_0 is 0.47 $cm^3\ g^{-1}$. With KOH in aqueous solution, alkaline hydrolysis of PET occurs and only macroporosity develops. The presence of surface hydroxyl and quinone type groups has been detected in AC samples, pH_{pzc} ranging between 5.35 and 7.20. The data of BPA adsorption fit better to the Ho and Mckay second order kinetic model than to the Lagergren first order model and to the Langmuir equation than to the Freundlich equation. The kinetic constant k_2 is 526 g $mol^{-1}\ h^{-1}$ and the equilibrium parameter Q_0 is 4.25 x 10^{-3} mol g^{-1} for SK1:5.

Acknowledgements. Financial support from the Junta de Extremadura through European Funds for Regional Development (ERDF) by the Aid to Research Groups (GR18013) is gratefully acknowledged.

Compliance with ethical standards

Conflict of interest The authors declare that they have no conflict of interest.

References

Adibfar M, Kaghazchi T, Asasian N, Soleimani M. (2014) Conversion of poly(ethylene terephthalate) waste into activated carbon: chemical activation and characterization. Chem Eng Technol 37 (6): 979-986. https://doi.org/10.1002/ceat.201200719

Almazán-Almazán MC, Pérez-Mendoza M, López-Domingo FJ, Fernández-Morales I, Domingo-García M, López-Garzón FJ (2007) A new method to obtain microporous carbons from PET: characterization by adsorption and molecular simulation. Micropor Mesopor Mat 106 (1-3):219-228. https://doi.org/10.1016//j.micromeso.2007.02.053

520 Andaluri G, Manickavachagam M (2018) Plastic toys as a source of exposure to bisphenol-A
521 and phthalates at childcare facilities. Environ Monit Assess 190:65.
522 https://doi.org/10.1007/s10661-017-6438-9

523 Arenillas A, Rubiera F, Parra, JB, Ania CO, Pis JJ (2005 Surface modification of low cost
524 carbons for their application in the environmental protection. Appl Surf Sci 252 (3): 619-624.
525 https://doi.org/10.1016//j.apsusc.2005.02.076

526 Bautista-Toledo I, Ferro-García MA, Rivera-Utrilla J, Moreno-Castilla C, Vegas Fernández FJ
527 (2014) Bisphenol A removal from water by activated carbon. Effects of carbon characteristics
528 and solution chemistry. Environ. Sci. Technol 39:6246-6250.
529 https://doi.org/10.1021/es0481169

530 Bautista-Toledo MI, Rivera-Utrilla J, Ocampo-Pérez R, Carrasco-Marín F, Sánchez-Polo M
531 (2014) Cooperative adsorption of bisphenol-A and chromium (III) ions from water on activated
532 carbons prepared from olive-mill waste. Carbon 73:338-350.
533 https://doi.org/10.1016//j.carbon.2014.02.073

534 Bazargan A, Hui CW, Mckay G (2013) Porous carbons from plastic waste. Adv Polym Sci
535 https://doi.org/10.1007/12_2013_253

536 Bohdziewicz J, Liszczyk G (2013) Evaluation of effectiveness of bisphenol A removal on
537 domestic and foreign activated carbons. Ecol Chem Eng S 20(2):371-379.
538 https://doi.org/10.2478/eces-2013-00273

539 Bóta A, László, K, Nagy LG, Copìtzky T (1997) Comparative study of active carbons from
540 different precursors. Langmuir 13:6502-6509. https://doi.org/10.1021//La9700883

541 Bratek W, Swiatkowski A, Pakula M, Biniak S, Bystrzejewski M, Szmigielski R (2013)
542 Characteristics of activated carbon prepared from waste PET by carbon dioxide activation. J
543 Anal Appl Pyrol 100:192-198. https://doi.org./10.1016//j.jaap.2012.12.021

544 Brems A, Baeyens J, Vandecasteele C, Dewil R (2011) Polymeric cracking of waste
545 polyethylene terephthalate to chemicals and energy. J Air & Waste Manage Assoc 61:721-731.
546 https://doi.org/10.3155/1047-3289.61.7.721

547 Colin A, Bach C, Rosin C, Munoz JF, Dauchy X (2014) Is drinking water a major route of
548 human exposure to alkylphenol and bisphenol contaminants in France?. Arch Environ Contam
549 Toxicol 66: 86-99. https://doi.org/10.1007/s00244-013-9942-0

550 Cousins IT, Staples CA, Klecka GM, Mackay D (2002) A multimedia assessment of the
551 environmental fate of bisphenol A. Hum Ecol Risk Assess 8:1107–1135.
552 https://doi.org/10.1080/1080-700291905846

553 Crain DA, Eriksen M, Iguchi T, Jobing S, Laufer H, LeBlanc GA, Guillette Jr LJ (2007) An
554 ecological assessment of bisphenol-A: evidence from comparative biology. Reprod Toxicol
555 24:225-239. https://doi.org/10.1016/reprotox.2007.05.008

556 Cwiek-Ludwicka KC (2015) Bisphenol A (BPA) in food contact materials – new scientific
557 opinion from EFSA regarding public health risk. Rocz Panstw Zakl Hig 66:299-307

558 Dias JM, Alvim-Ferraz MCM, Almeida MF, Rivera-Utrilla J, Sanchez-Polo M (2007) Waste
559 materials for activated carbon preparation and its use in aqueous phase treatment: a review. J
560 Environ Manage 85:833–846. https://doi.org/10.1016/j.jenvman.2007.07.031

561 Djahed B, Shahsavani E, Naji FK, Mahvi AH (2015) A novel and inexpensive method for
562 producing activated carbon from waste polyethylene terephthalate bottles and using it to remove
563 methylene blue dye from aqueous solution. Desalin Water Treat
564 https://doi.org/10.1080/19443994.2015.1033647

565 Dong Y, Wu D, Chen X, Lin Y (2010) Adsorption of bisphenol A from water by surfactant-
566 modified zeolite. J Colloid Interface Sci 348:585-590.
567 https://doi.org/10.1016/j.jcis.2010.04.074

568 Dubinin MM (1975) Physical adsorption of gases and vapors in micropores. In: Cadenhead
569 DA, Danielli JF, Rosenberg MD (eds.) Progress in Surface and Membrane Science. Academic
570 Press, New York, pp 1-70
571 Durán-Valle CJ, Gómez-Corzo M, Pastor-Villegas J, Gómez-Serrano V (2005) Study of cherry
572 stones as raw material in preparation of carbonaceous adsorbents. J Anal Appl Pyrolysis 73:59-
573 67. https://doi.org/10.1016/j.jaap.2004.10.004
574 Dwivedi AD, Gopal K, Jain R (2011) Strengthening adsorption characteristics of non-steroidal
575 anti-inflammatory drug onto microwave-assisted mesoporous material: process design,
576 mechanism and characterization. Chem Eng J 168:1279-1288.
577 https://doi.org/10.1016/j.cej.2011.02.041
578 Esfandiari A, Kaghazchi T, Soleimani M (2012) Preparation and evaluation of activated
579 carbons obtained by physical activation of polyethyleneterephthalate (PET) wastes. J Taiwan
580 Inst Chem Eng 43 (4):631-637. https://doi.org/10.1016/j.jtice.2012.02.002
581 Fernández-Morales I, Almazán-Almazán MC, Pérez-Mendoza M, Domingo-García M, López-
582 Garzón FJ (2005) PET as precursor of microporous carbons: preparation and characterization.
583 Micropor Mesopor Mat 80:107–115. https://doi.org/10.1016/j.micromeso.2004.12.006
584 Giles C.H, MacEwan TH, Nakhwa SN, Smith D (1960) Studies in adsorption. Part XI. A system
585 of classification of solution adsorption isotherms, and its use in diagnosis of adsorption
586 mechanisms and in measurement of specific surface areas of solids. J Chem Soc London 3973-
587 3993
588 Gregg SJ, Sing KSW (1982) Adsorption, surface area and porosity. Academic Press
589 Han W, Luo L, Zhang S (2012) Adsorption of bisphenol A on lignin: effects of solution
590 chemistry. Int J Environ Sci Technol 9:543-540. https://doi.org/10.1007/s13762-012-0067-1

591 Hermabessiere L, Dehaut A, Paul-Pont I, Lacroix C, Jezequel R, Soudant P, Duflos G (2017)
592 Occurrence and effects of plastic additives on marine environments and organisms: a review.
593 Chemosphere 182:781-793. https://doi.org/10.1016/j.chemosphere.2017.05.096
594 Ho YS, McKay G (1999) Pseudo-second order model for sorption processes. Biochem 34:451-
595 465. https://doi.org/10.1016/S0032-9592(98)00112-5
596 Jafer M, Ibrahim H, Taufiq-Yap Y.H (2019) Bisphenol A removal from aqueous solution using
597 waste agarwood activated carbon: kinetic and isotherm investigation of adsorption process.
598 Eurasian J Anal Chem 14(4):32-41
599 Ji LN (2013) Study on preparation process and properties of polyethylene terephthalate (PET).
600 App Mech Mater 312:406-410. https://doi.org/10.4028/www.scientific.net/AMM.312.406
601 Kamaraj M, Manjudevi M, Sivaraj R (2012) Degradation of bisphenol A by *Aspergillus* Sp.
602 isolated from tannery industry effluent. Int J Pharm & Life Sci 3(4):1585-1589
603 Karayannidis GP, Chatziavgoustis AP, Achilias DS (2002) Poly(ethylene terephthalate)
604 recycling and recovery of pure terephthalic acid by alkalyne hydrolysis. Adv Polym Technol
605 21:250-259. https://doi.org/10.1002/adv.10029
606 Kartel NT, Gerasimenko NV, Tsyba NN, Nikolaichuk AD, Kovtun GA (2001) Synthesis and
607 study of carbon sorbent prepared from polyethylene terephthalate. Russ J Appl Chem 74
608 (10):1765–1767
609 Kaufman D, Wright G, Kroemer R, Engel J (1999) “New” compounds from old plastics:
610 recycling PET plastics via depolymerization. J Chem Educ 76 (11):1525-1526.
611 https://doi.org/10.1021/ed076p1525
612 Kumar S, Guria C (2005) Alkaline hydrolysis of waste poly(ethylene terephthalate): a modified
613 shrinking core model. J Macromol Sci Part A. https://doi.org/10.1081/MA-200050346
614 Laing IV, Viana J, Dempster EL, Trznadel M, Trunkfield LA, Uren Webster TM, van Aerle R,
615 Paull GC, Wilson RJ, Mill J, Santos EM. (2016) Bisphenol A causes reproductive toxicity,

616 decreases dnmt1 transcription, and reduces global DNA methylation in breeding zebrafish
617 (Danio rerio). Epigenetics 11 (7):526-538. https://doi.org/10.1080/15592294.2016.1182272
618 László K, Bóta A, Nagy LG, Cabasso I (1999) Porous carbons from polymer waste materials.
619 Colloids Surf A 151:311-320. https://doi.org/10.1016/S0927-7757(98)00390-2
620 Le HH, Carlson EM, Chua JP, Belcher SM (20089 Bisphenol A is released from polycarbonate
621 drinking bottles and mimics the neurotoxic actions of estrogen in developing cerebellar
622 neurons. Toxicol Lett 176 (2):149-156. https://doi.org/10.1016/j. toxlet.2007.11.001

623 Lin Z, Wang L, Jia Y, Zhang Y, Dong Q, Zhang Y, Don Q, Huang C (2017) A study on
624 environmental bisphenol A pollution in plastics industry areas. Water Air Soil Pollut 228:98.
625 https://doi.org/10.1007/s11270-017-3277-9

626 Liu G, Ma J, Li X, Qin Q (2009) Adsorption of bisphenol A from aqueous solution onto
627 activated carbons with different modification treatments. J Hazard Mater 164 (2-3):1275–1280.
628 https://doi.org/10.1016/j.jhazmat.2008.09.038
629 Liu G, Li X, Campos LC (2017) Role of the functional groups in the adsorption of bisphenol A
630 onto activated carbon: thermal modification and mechanism. J Water Supply Res T 66(2):105-
631 115
632 Marzec M, Tryba B, Kalenczuk RJ, Morawski AW (1999) Poly(ethylene terephthalate) as a
633 source for activated carbon. Polym Adv Technol 10:588–595
634 Mendoza-Carrasco R, Cuerda-Correa EM, Alexandre-Franco MF, Fernández–González C,
635 Gómez-Serrano, V (2016) Preparation of high-quality activated carbon from
636 polyethyleneterphthalate (PET) bottle waste. Its use in the removal of pollutants in aqueous
637 solution. J Environ Manage 181:522-535. https://doi.org/10.1016/j.jenvman.2016.06.070
638 Nakagawa K, Namba A, Mukai SR, Tamon H, Ariyadejwanich P, Tanthapanichakoon W
639 (2004) Adsorption of phenol and reactive dye from aqueous solution on activated carbons

derived from solid wastes. Water Res 38 (7):1791–1798. https://doi.org/10.1016/j.watres.2004.01.002

Olivares-Marín M, Fernández-González C, Macías-García A, Gómez-Serrano V (2007) Porous structure of activated carbon prepared from cherry stones by chemical activation with phosphoric acid. Energ Fuel. 21 (5):2942-2949. https://doi.org/10.1021/ef060652u

Palme A, Peterson A, de la Motte H, Theliander H, Brelid H (2017) Development of an efficient route for combined recycling of PET and cotton from mixed fabrics. Text Clothing Sustain. https://doi.org/10.1186/s40689-017-0026-9

Parra JB, Ania CO, Arenillas A, Pis JJ (2002) Textural characterization of activated carbons obtained from poly(ethylene terephthalate) by carbon dioxide activation. Stud Surf Sci Catal 144:537–543. https://doi.org/10.1016/S0167-2991(02)80178-1

Paszun D, Spychaj T (1997) Chemical recycling of poly(ethylene terephthalate). Ind Eng Chem Res 36 (4):1373-1383. https://doi.org/10.1021/ie960563c

Pellera FM, Giannis A, Kalderis D, Anastasiadou K, Stegmann R, Wang, JY, Gidarakos E (2012) Adsorption of Cu(II) ions from aqueous solutions on biochars prepared from agricultural by–products. J Environ Manage 96 (1):35–42. https://doi.org/10.1016/j.jenvman.2011.10.010

PlasticsEurope, Plastics - the Facts 2018. Plastics the facts 2018- AFweb.pdf

Radovic LR, Moreno-Castilla C, Rivera-Utrilla J (2001) Materials as adsorbents in aqueous solutions. In: Radovic LR (ed.) Chemistry and Physics of Carbon. Marcel Dekker, New York, pp 227–405

Rahmat NA, Hadibarata T, Yuniarto A, Elshikh MS, Syafiudding A (2019) Isotherm and kinetics studies for the adsorption of bisphenol A from aqueous solution by activated carbon of *Musa acuminata*. IOP Conf. Series: Materials Science and Engineering 495:012059. https://doi.org/10.1088/1757-899X/495/1/012059

664 Rani M, Shim WJ, Han GM, Jang M, Al-Odaini NA, Song YK, Hong SH (2015) Qualitative
665 analysis of additives in plastic marine debris and its new products. Arch Environ Contam
666 Toxicol 69:352-366. https://doi.org/10.1007/s00244-015-0224-x
667 Recycling International. PET consumption to exceed 20 million tonnes by 2021 (2016)
668 Rochester JR (2013) Bisphenol A and human health: a review of the literature. Reprod Toxicol
669 42:132-155. https://doi.org/10.1016/j.reprotox.2013.08.008
670 Rykowska I, Wasiak W (2006) Properties, threats, and methods of analysis of bisphenol A and
671 its derivatives. Acta Chromatogr 16:7-27

672 Santhi VA, Sakai N, Ahmad ED, Mustafa AM (2012) Occurrence of bisphenol A in surface
673 water, drinking water and plasma from Malaysia with exposure assessment from consumption
674 of drinking water. Sci Total Environ 427–428-332–338. https://doi.org/
675 10.1016/j.scitotenv.2012.04.041

676 Schäfer AI, Nghiem LD, Oschmann N (2006) Bisphenol A retention in the direct ultrafiltration
677 of greywater. J Membr Sci. https://doi.org/10.1016/j.memsci.2006.06.035

678 Smisek M, Cerny S (1970) Active carbon: manufacture, properties and applications. Elsevier

679 Spaseska D, Civkaroska M (2010) Alkaline hydrolysis of poly(ethylene terephthalate) recycled
680 from the postconsumer soft-drink bottles. J Univ Chem Technol Metal 45 (4):379-384

681 Staples CA, Dorn PB, Klecka GM, O´Block ST, Harris LR (1998) A review on the
682 environmental fate, effects, and exposures of bisphenol A. Chemosphere 36 (10): 2149-2473.
683 https://doi.org/10.1016/s0045-6535(97)10133-3

684 Supong A, Bhomick PC, Baruah M, Pongener C, Sinha UB, Sinha D (2019) Adsorptive
685 removal of Bisphenol A by biomass activated carbon and insights into the adsorption

686 mechanism through density functional theory calculations. Sustain Chem Pharm 13:100159.
687 https://doi.org/10.1016/j.scp.2019.100159

688 Sych NV, Kartel NT, Tsyba NN, Strelko VV (2006) Effect of combined activation on the
689 preparation of high porous active carbons from granulated post-consumer
690 polyethyleneterephthalate. Appl Surf Sci 252:8062-8066. https://doi.org/10.1016/j.apsusc-
691 2005.10.009

692 Tay KS, Rahman NA, Abas, MRB (2012) Degradation of bisphenol A by ozonation: rate
693 constants, influence of inorganic anions, and by-products. Maejo Int J Sci Technol 6 (01): 77-
694 94

695 Tsai WT, Lai CW, Su TS (2006) Adsorption of bisphenol-A from aqueous solution onto
696 minerals and carbon adsorbents. J Hazard Mater B134:169-175.
697 https://doi.org/10.1016/j.hazmat.2005.10.055

698 Wagner M, Oehlmann J (2009) Endocrine disruptors in bottled mineral water: total estrogenic
699 burden and migration from plastic bottles. Environ Sci Pollut Res 16: 278-286.
700 https://doi.org/10.1007/s11356-009-0107-7

701 Wan BZ, Kao CY, Cheng WH (2001) Kinetics of depolymerization of poly(ethylene
702 terephthalate) in a potassium hydroxide solution. Ind Eng Chem Res 40 (2): 509-514.
703 https://doi.org/10.1021/ie0005304

704 Weber TW, Chakravorti RK (1974) Pore and solid diffusion models for fixed-bed adsorbers.
705 AIChE J 20:228-238. https://doi.org/10.1002/aic.690200204

706 Wirasnita R, Hadibarata T, Yusoff ARM, Yusop Z (2014) Removal of bisphenol A from
707 aqueous solution by activated carbon derived from oil palm empty fruit bunch. Water Air Soli
708 Pollut 222:2148. https://doi.org/10.1007//s11270-014-2148-x

709 Yamamoto T, Yasuhara A, Shiraishi H, Nakasugi O (2001) Bisphenol A in hazardous waste
710 landfill leachates. Chemosphere 42 (4):415–418. https://doi.org/10.1016/s0045-
711 6535(00)00079-5
712 Zielinska M, Wojnowska-Baryla I, Cydzik-Kwiatkowska, A (2019) Bisphenol A removal from
713 water and wastewater. Springer
714 Yamashita M, Mukai H (2011) Alkaline hydrolysis of polyethylene terephthalate at lower
715 reaction temperature. Sci Eng Rev Doshisha Univ 52 (2):51-56
716
717
718

Table Headings

Table 1. Preparation of AC from PET by physical and chemical activation methods. Process yield and sample notations

Table 2. Textural characterization of AC by the N_2 adsorption at -196ºC. Surface area and pore volumes

Table 3. Textural characterization of AC by mercury porosimetry and density measurements. Pore volumes and mercury densities

Table 4. pH_{pzc} values for the AC samples

Table 5. FT-IR spectrum of BPA

Table 6. BPA adsorption. Fitting of kinetic data to pseudo-first and pseudo-second order models

Table 7. BPA adsorption. Fitting of isotherms to the Freundlich and Langmuir equations

Table 8. Comparison of the Langmuir adsorption capacity of BPA for a PET-derived AC and other ACs.

Captions to figures

Fig. 1. Molecular structure of PET

Fig. 2. Molecular structure of BPA

Fig. 3. Adsorption isotherms of N_2 at -196 °C

Fig. 4. Curves of mercury intrusion

Fig. 5. FT-IR spectra for selected AC samples

Fig. 6. pH_{pzc} measurement

Fig. 7. FT-IR spectra of BPA, SK1:5 and SK1:5-BPA

Fig. 8. Adsorption kinetics of BPA for selected AC samples

744 **Fig. 9.** Adsorption isotherms of BPA for selected AC samples

745
746

Table 1

Preparation of AC from PET by physical and chemical activation methods. Process yield and sample notations

Aa	I_p	I_T/ºC	I_t/h	T/ºC	S_t/h	I_Y/%	A_Y/%	Notation
Steam	-	-	-	900	1	-	5.9	WV
KOH	1:1	85	2	850	2	96.0	58.4	LK1:1
KOH	1:3	85	2	850	2	93.1	48.3	LK1:3
KOH	1:5	85	2	850	2	75.8	49.4	LK1:5
KOH	1:1	-	-	850	2	-	75.8	SK1:1
KOH	1:3	-	-	850	2	-	38.1	SK1:3
KOH	1:5	-	-	850	2	-	23.9	SK1:5

Abbreviations: Aa, activating agent; I_p, impregnation ratio (PET:KOH); I_T, impregnation treatment temperature; I_t, impregnation treatment time; T, maximum heat treatment temperature (MHTT); S_t, soaking time at MHTT; I_Y, impregnation process yield; A_Y, activation process yield.

Table 2

Textural characterization of AC by the N_2 adsorption at -196ºC. Surface area and pore volumes

Sample	$S_{BET}/m^2\ g^{-1}$	$W_0/cm^3\ g^{-1}$	$V_{mi}/cm^3\ g^{-1}$	$V_{me}/cm^3\ g^{-1}$
WV	1061	0.47	0.49	0.34
LK1:1	125	0.06	0.05	0.07
LK1:3	27	0.01	0.01	0.04
LK1:5	12	0.00	0.00	0.03
SK1:1	1060	0.41	0.42	0.19
SK1:3	1564	0.58	0.60	0.27
SK1:5	1990	0.71	0.55	0.73

From the N_2 adsorption isotherm: S_{BET}, specific surface area (BET equation; $p/p^0 = 0.05$-0.30, am = 16.2 Å^2); W_0, micropore volume (Dubinin-Radushkevich equation); V_{mi}, micropore volume (V_{ad} at $p/p^o = 0.10$, V_{ad} = volume adsorbed); V_{me}, mesopore volume (V_{ad} at $p/p^o = 0.95$ and at $p/p^o = 0.10$).

Table 3

Textural characterization of AC by mercury porosimetry and density measurements. Pore volumes and mercury densities

Sample	$V_{me\text{-}p}/cm^3\ g^{-1}$	$V_{ma\text{-}p}/cm^3\ g^{-1}$	$\rho_{Hg}/g\ cm^{-3}$	$\rho_{Hg}^{-1}/cm^3\ g^{-1}$	$V'_T/cm^3\ g^{-1}$
WV	0.36	0.08	1.24	0.81	0.91
LK1:1	0.13	0.38	0.87	1.15	0.57
LK1:3	0.10	0.35	0.99	1.01	0.46
LK1:5	0.08	0.35	0.95	1.05	0.43
SK1:1	0.31	1.49	0.40	2.50	2.21
SK1:3	0.56	2.11	0.31	3.23	3.25
SK1:5	0.81	1.77	0.35	2.86	3.29

From the curves of mercury intrusion: $V_{me\text{-}p}$, mesopore volume; $V_{ma\text{-}p}$, macropore volume. ρ_{Hg}, mercury density; V'_T, total pore volume ($W_0 + V_{me\text{-}p} + V_{ma\text{-}p}$).

Table 4

pH_{pzc} values for the AC samples

Sample	pH_{pzc}
WV	7.20
LK1:1	6.35
LK1:3	6.37
LK1:5	6.25
SK1:1	5.60
SK1:3	5.35
SK1:5	5.70

Table 5

FT-IR spectrum of BPA

Band position/cm^{-1}	Bond vibration	Atomic grouping
3449	ν(O-H)	H-bonded phenolic OH
2962	ν_a(C-H)	CH_3
2879	ν_s(C-H)	CH_3
1607	ν(C=C) skeletal	Aromatic ring
1502	ν(C=C) skeletal	Aromatic ring
1443	δ_a(C-H)	CH_3
1377	δs(C-H)	CH_3
1232	ν(C-O)	Phenolic OH
1074	ν(C-C), δ(C-H)	Aromatic ring
827	γ(C-H)	1,4-Disubstituted aromatic ring

Symbols: ν, stretching; δ, bending (in-plane); γ, bending (out-of-plane); a, asymmetrical; s, symmetrical.

778

779 **Table 6**

780 BPA adsorption. Fitting of kinetic data to pseudo-first and pseudo-second order models

		Pseudo-first order				Pseudo-second order		
Sample	t_e/h	$q_{e(theoretical)}\cdot10^4$/ mol g^{-1}	$q_e\cdot10^4$/ mol g^{-1}	k_1/ h^{-1}	R^2	$q_e\cdot10^4$/ mol g^{-1}	k_2/ g mol^{-1} h^{-1}	R^2
WV	100	19.66	17.37	0.04	0.9841	20.64	59	0.9920
SK 1:1	100	12.22	6.98	0.03	0.914	12.52	258	0.9960
SK 1:3	100	22.83	9.47	0.03	0.9082	22.87	222	0.9980
SK 1:5	100	21.99	5.48	0.02	0.7191	22.08	526	1.000

781 Abbreviations: t_e, equilibrium time; q_e, amounts adsorbed at equilibrium; k_1, pseudo-first order
782 rate constant; k_2, rate constant of pseudo-second order adsorption; R^2, fitting coefficient.

783
784
785 **Table 7**
786 BPA adsorption. Fitting of isotherms to the Freundlich and Langmuir equations

	Langmuir					Freundlich	
Sample	$Q_0\cdot10^3$/ mol g^{-1}	$b\cdot10^{-3}$/ L mol^{-1}	R_L	R^2	1/n	$K_F\cdot10^3$/ (mol g^{-1})/(mol L^{-1})$^{1/n}$	R^2
WV	2.62	15.60	0.060	0.9980	0.50	118.88	0.6147
SK1:1	1.11	8.50	0.105	0.4462	2.37	-	0.6577
SK1:3	2.15	84.71	0.012	0.9980	0.10	4.39	0.9467
SK1:5	4.25	10.84	0.084	1.000	0.26	25.51	0.9663

787 Abbreviations: Q_0, maximum monolayer coverage capacity; b, Langmuir isotherm constant; n,
788 adsorption intensity; K_F, Freundlich isotherm constant; R^2, fitting coefficient.

789

Table 8

Comparison of the Langmuir adsorption capacity of BPA for a PET-derived AC and other ACs.

AC	S_{BET}/ $m^2\ g^{-1}$	V_{mi}/ $cm^3\ g^{-1}$	Vt/ $cm^3\ g^{-1}$	$Q_0 \cdot 10^3$/ $mol\ g^{-1}$	Reference
A	1225	0.563	1.088	1.00	
B	1084	0.496	0.789	1.15	
C	1216	0.505	0.725	1.04	Bautista-Toledo et al. 2005
D	916		0.576	1.44	
E	1060		0.714	1.15	Tsai et al. 2006
F	900		0.365	0.58	Bohdziewicz and Liszczyk 2013
G	1767	0.486	1.581	2.09	Liu et al. 2017
H	1092			1.92	Jafer et al. 2019
I	222-854		0.125-0.445	0.07	Supong et al. 2019
J				0.15	Rahmat et al. 2019
K	1990	0.710	3.290	4.25	This study

ACs were commercial: A, Sorbone Norit; B, Merck; D, Calgon Carbon Co. (coconut shell based-based), E, Calgon Carbon Co. (bituminous coal-based); F, Gryfskand (Poland); G, Westvsco, Corp., American; or synthetized products,

C: almond shells; 1000 ºC, 1 h, N_2; 850 ºC, 5 h, steam.

H: agarwood; 700 ºC, 1 h, N_2; 750 ºC, 4 h, CO_2.

I: *Tithonia diversifolia* (tree marigold); 600 ºC, 1 h; KOH, 0.5:1–3:1, 500-800 ºC, 2 h.

J: banana fronds: $ZnCl_2$, 10 %; 300 ºC, 1 h.

K: PET; KOH, 1:5; 850 ºC, 2 h.

Fig. 1. Molecular structure of PET

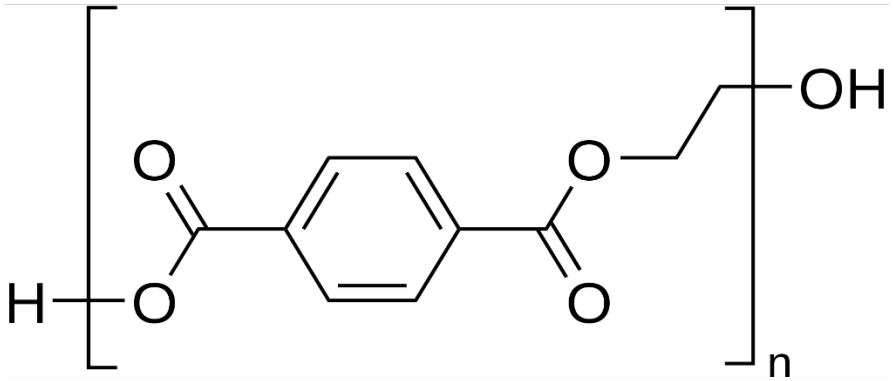

Fig. 2. Molecular structure of BPA

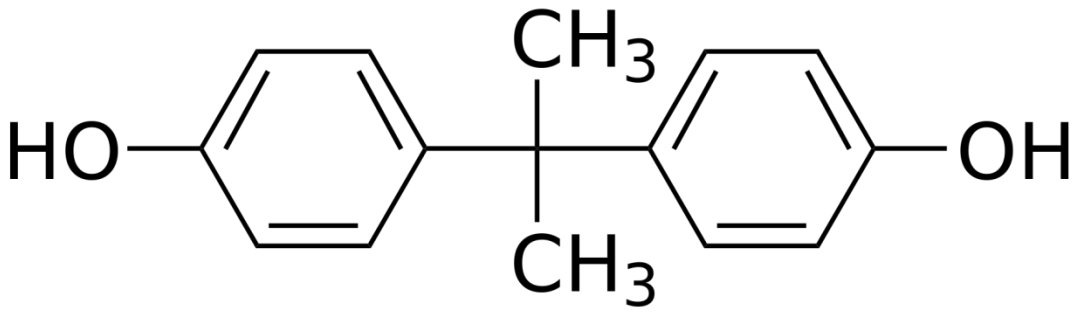

816 **Fig. 3.** Adsorption isotherms of N_2 at -196 °C

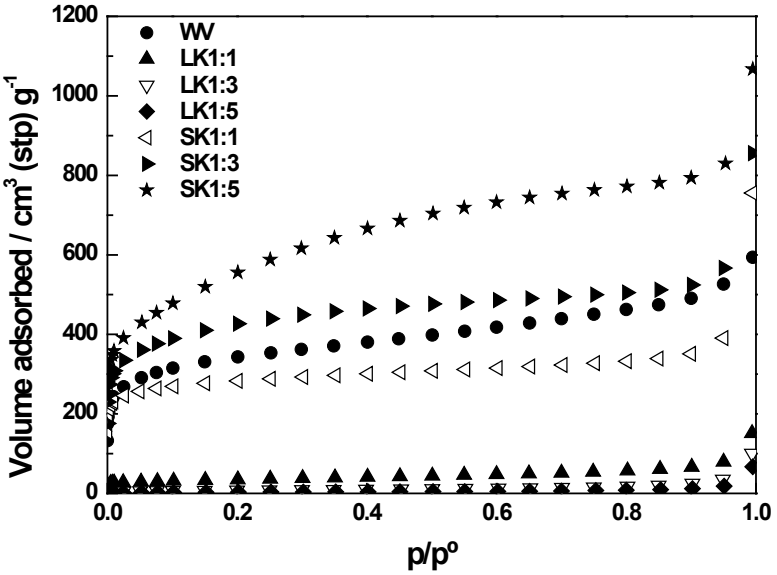

817

818

819 **Fig. 4.** Curves of mercury intrusion

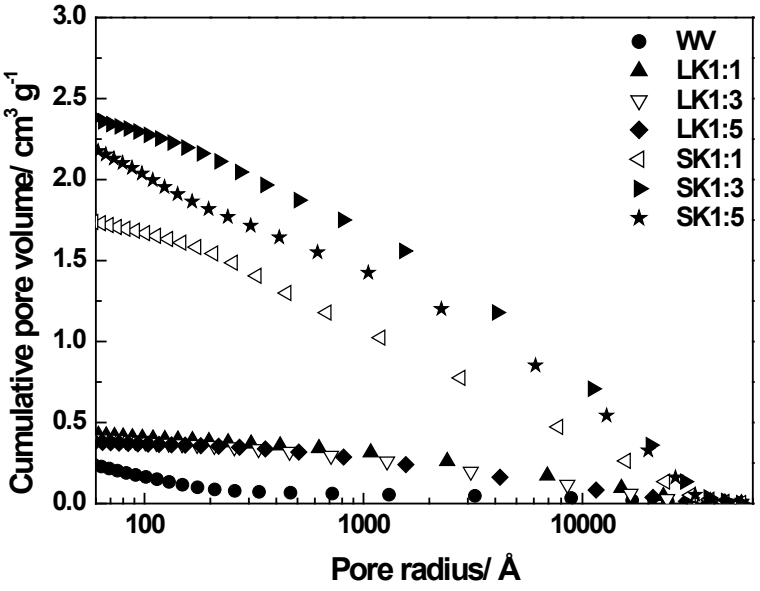

820

821

822

823 **Fig. 5.** FT-IR spectra for selected AC samples

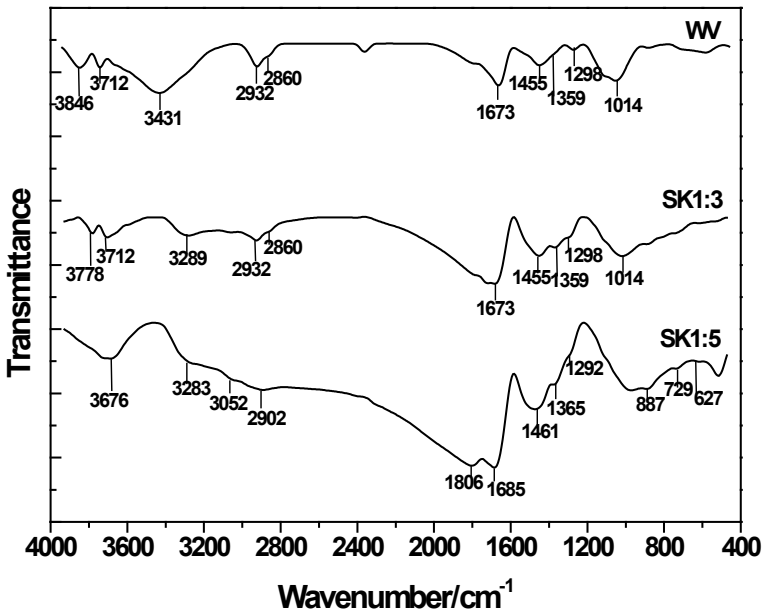

824

825

826

827 **Fig. 6.** pH_{pzc} measurement

828

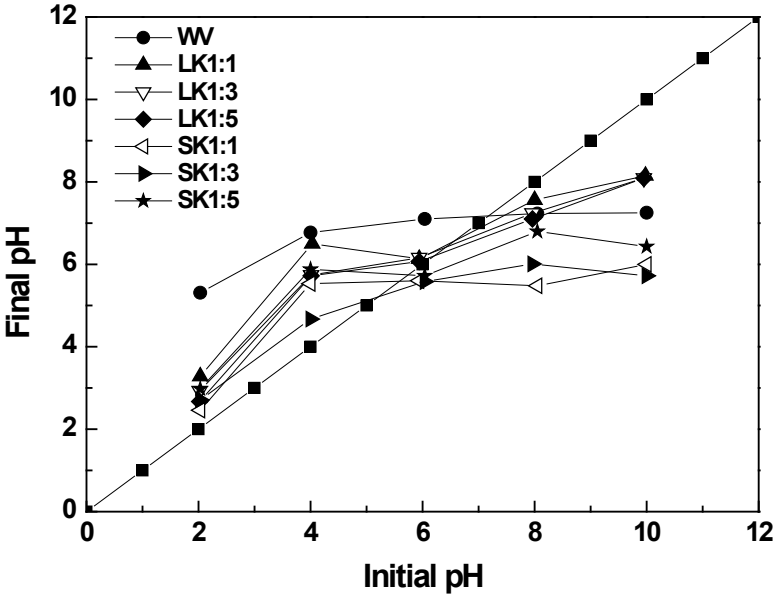

829

830

831 **Fig. 7.** FT-IR spectra of BPA, SK1:5 and SK1:5-BPA

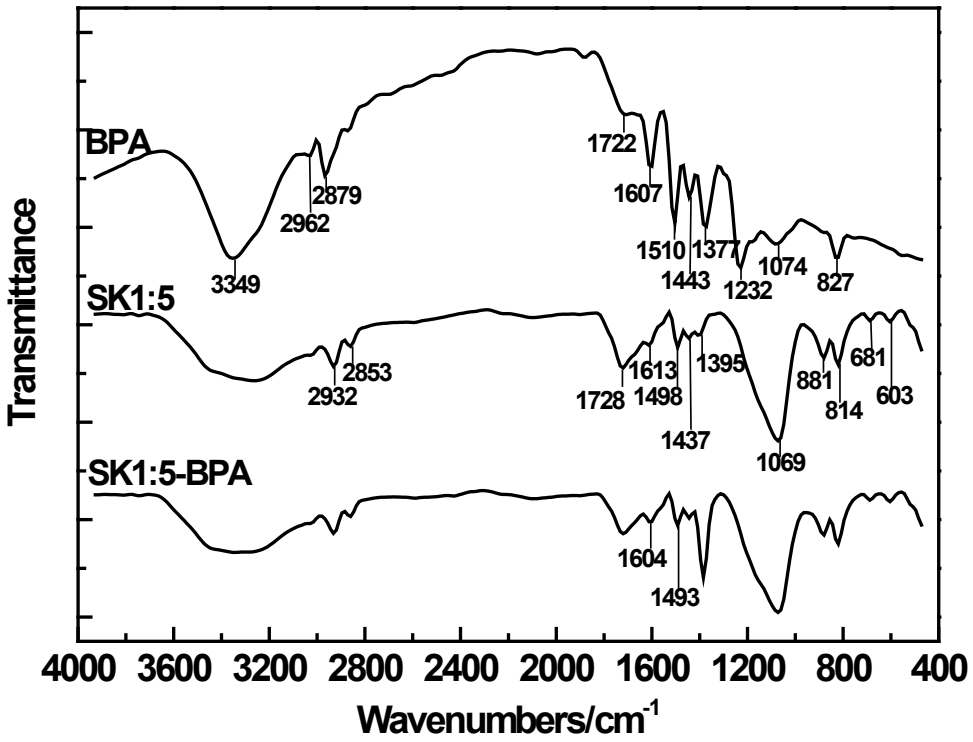

832

833

834 **Fig. 8.** Adsorption kinetics of BPA for selected AC samples

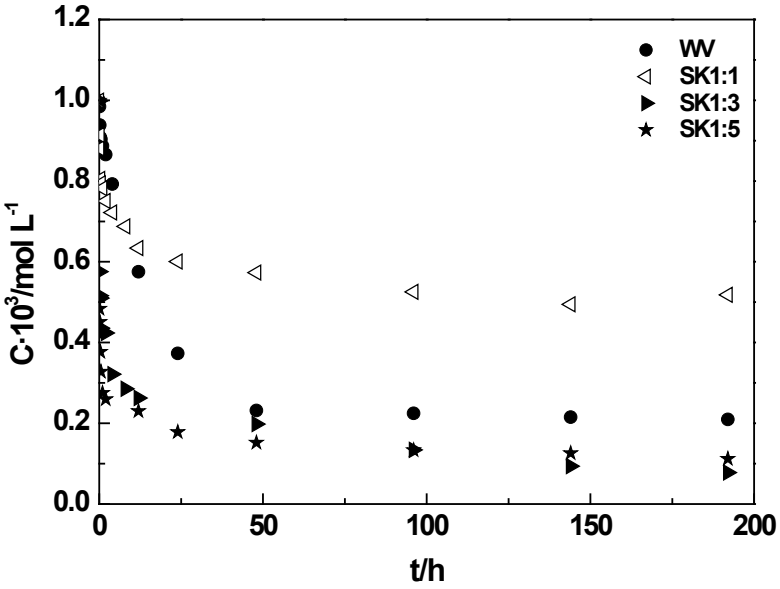

835

836

837 **Fig. 9.** Adsorption isotherms of BPA for selected AC samples

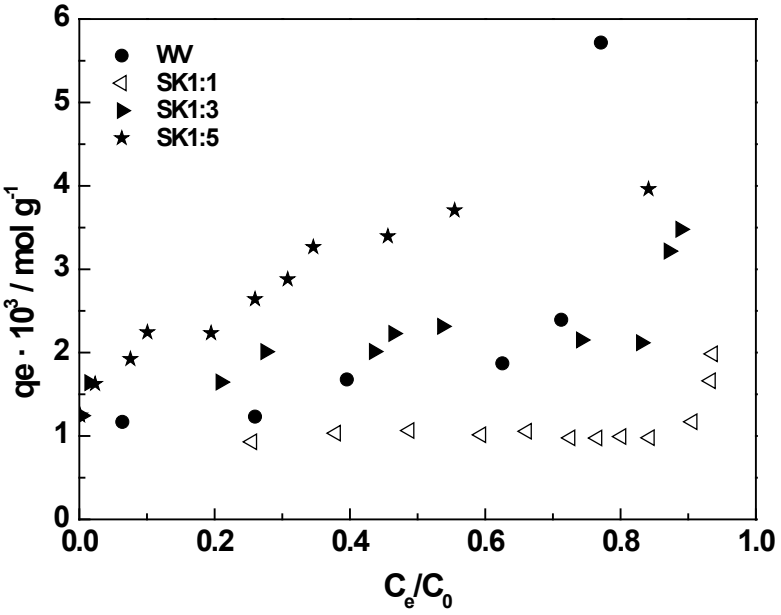

838

839

HIGHLIGHS

- The removal of two deleterious environmental pollutants as PET plastic bottles and BPA is studied.
- The activation of PET plastic with solid KOH entails AC with a highly developed porous structure.
- With such an AC as adsorbent, the adsorption process of BPA is fast and effective.
- The steam activation is less beneficial on the process yield, AC porous texture and BPA adsorption.